Electronic Supplementary Information

Preparation of Vibrational Quasi-Bound States of the Transition State Complex BrHBr from the Bihalide Ion BrHBr⁻

Luis H. Delgado-Granados[a], Carlos A. Arango[b], José G. López[*a]

[a] Departamento de Química, Universidad del Valle, A.A. 25360, Cali, Colombia. E-mail: jose.g.lopez@correounivalle.edu.co
[b] Departamento de Ciencias Químicas, Universidad Icesi, Cali, Colombia
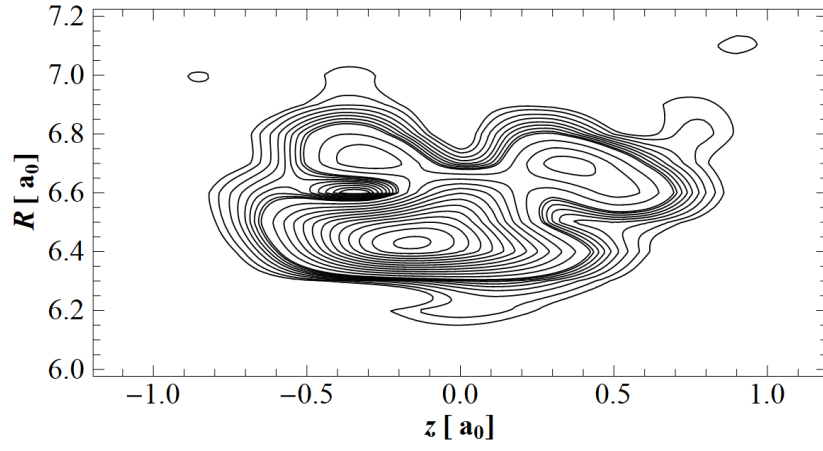
Figure S1: Squared modulus of the final state obtained under the interaction of the sequence of two LCPs, as described in Table 2(a).
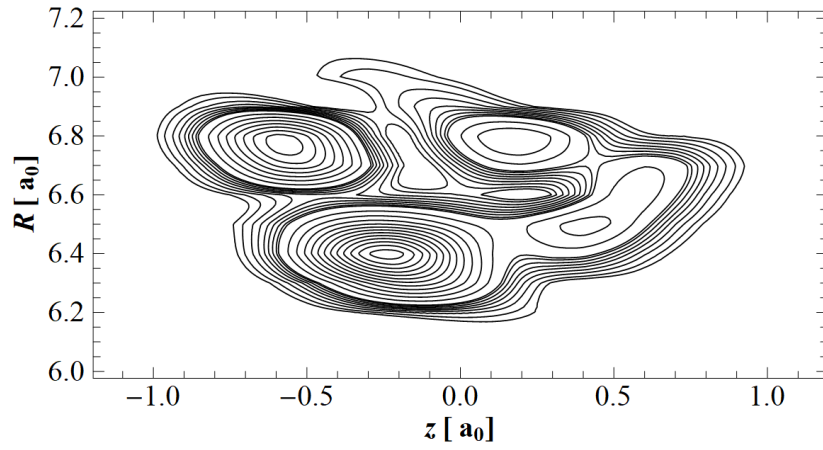
Figure S2: Squared modulus of the final state obtained under the interaction of the sequence of three LCPs, as described in Table 2(b).
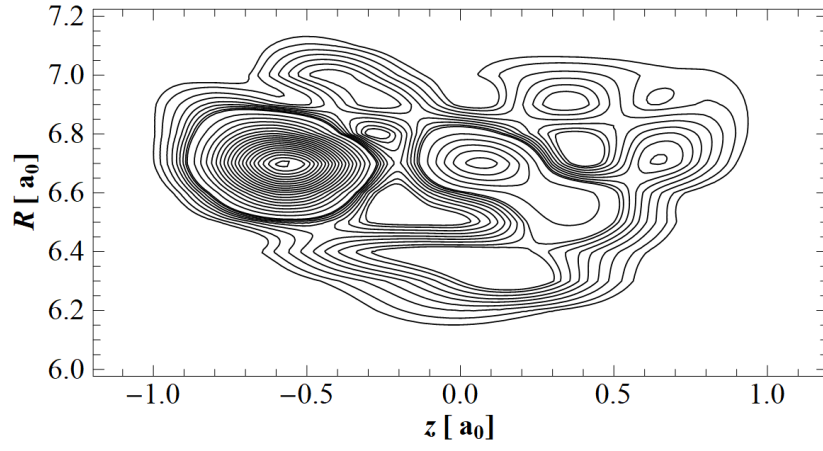
Figure S3: Squared modulus of the final state obtained under the interaction of the sequence of four LCPs, as described in Table 2(c).
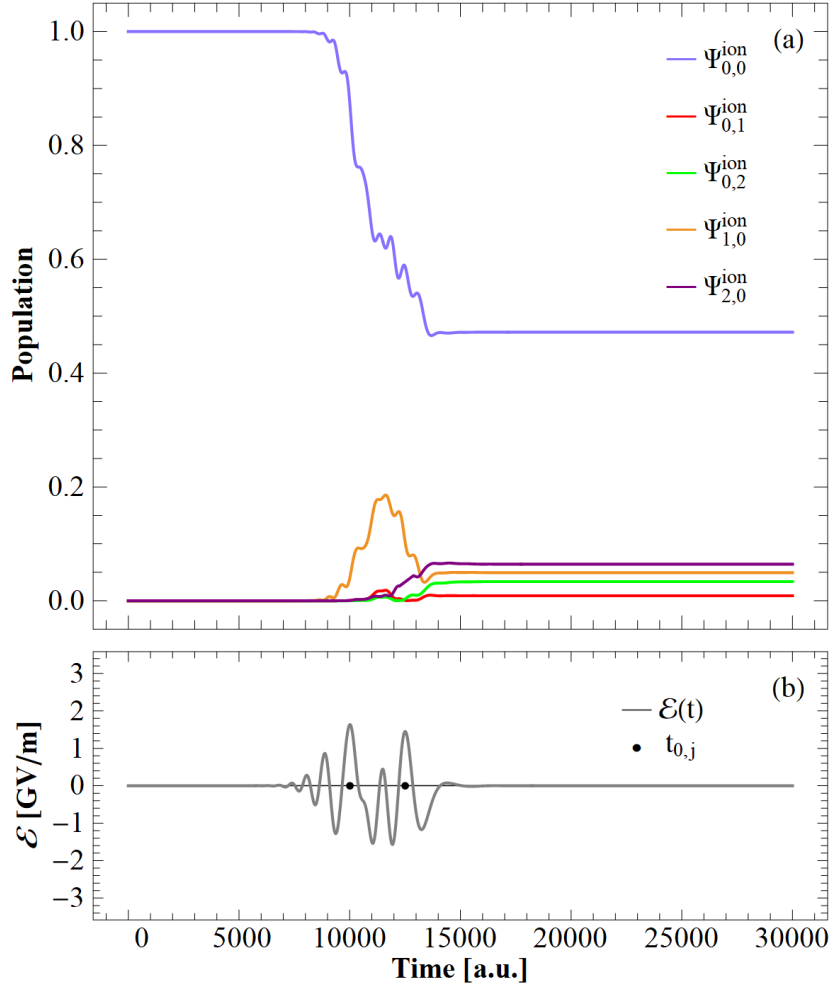
Figure S4: (a) Time evolution of the population of the vibrational eigenstates of $BrHBr^-$ $\Psi^{ion}_{0,0}$, $\Psi^{ion}_{1,0}$, $\Psi^{ion}_{0,1}$, $\Psi^{ion}_{2,0}$, and, $\Psi^{ion}_{0,2}$ under the interaction with a sequence of two LCPs. (b) Composite laser field sequence of two LCPs. The black dots on the horizontal axis show the time of the highest intensity value for each of the two LCPs, $t_{0,j}$, as described in Table 2(a).

5
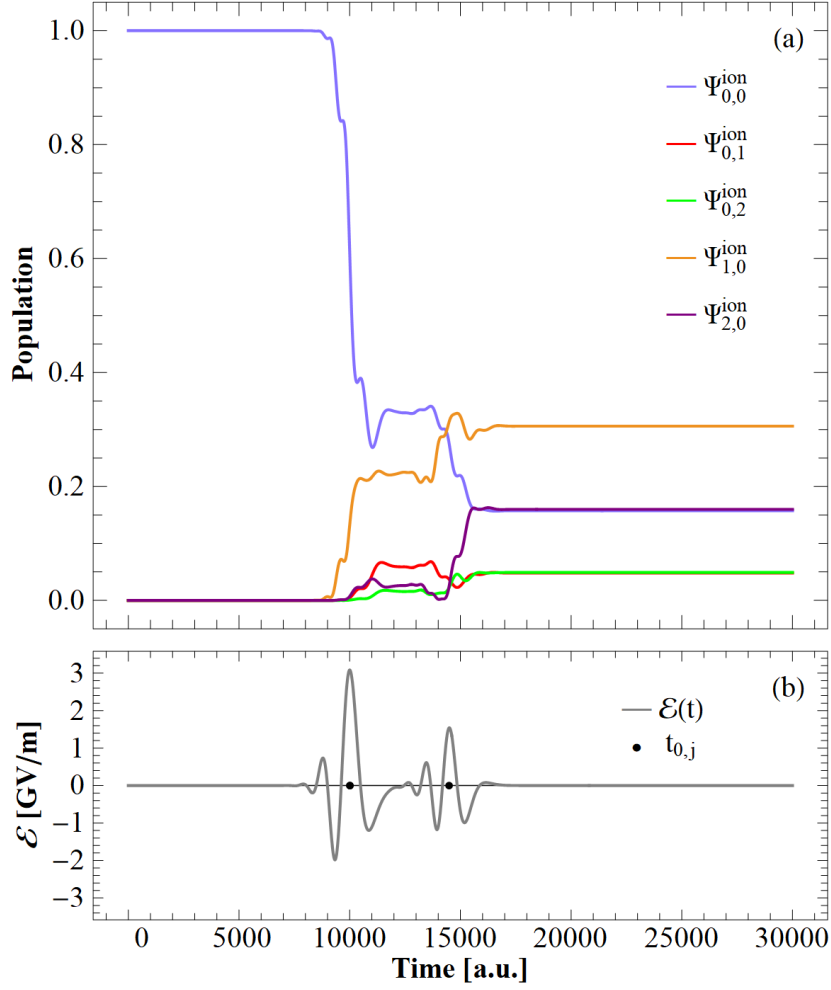
Figure S5: (a) Time evolution of the population of the vibrational eigenstates of BrHBr$^-$ $\Psi_{0,0}^{ion}$, $\Psi_{1,0}^{ion}$, $\Psi_{0,1}^{ion}$, $\Psi_{2,0}^{ion}$, and, $\Psi_{0,2}^{ion}$ under the interaction with a sequence of three LCPs. (b) Composite laser field sequence of three LCPs. The black dots on the horizontal axis show the time of the highest intensity value for each of the three LCPs, $t_{0,j}$, as described in Table 2(b).

Figure S6: (a) Time evolution of the population of the vibrational eigenstates of BrHBr$^-$ $\Psi_{0,0}^{ion}$, $\Psi_{1,0}^{ion}$, $\Psi_{0,1}^{ion}$, $\Psi_{2,0}^{ion}$, and, $\Psi_{0,2}^{ion}$ under the interaction with a sequence of four LCPs. (b) Composite laser field sequence of four LCPs. The black dots on the horizontal axis show the time of the highest intensity value for each of the four LCPs, $t_{0,j}$, as described in Table 2(c).
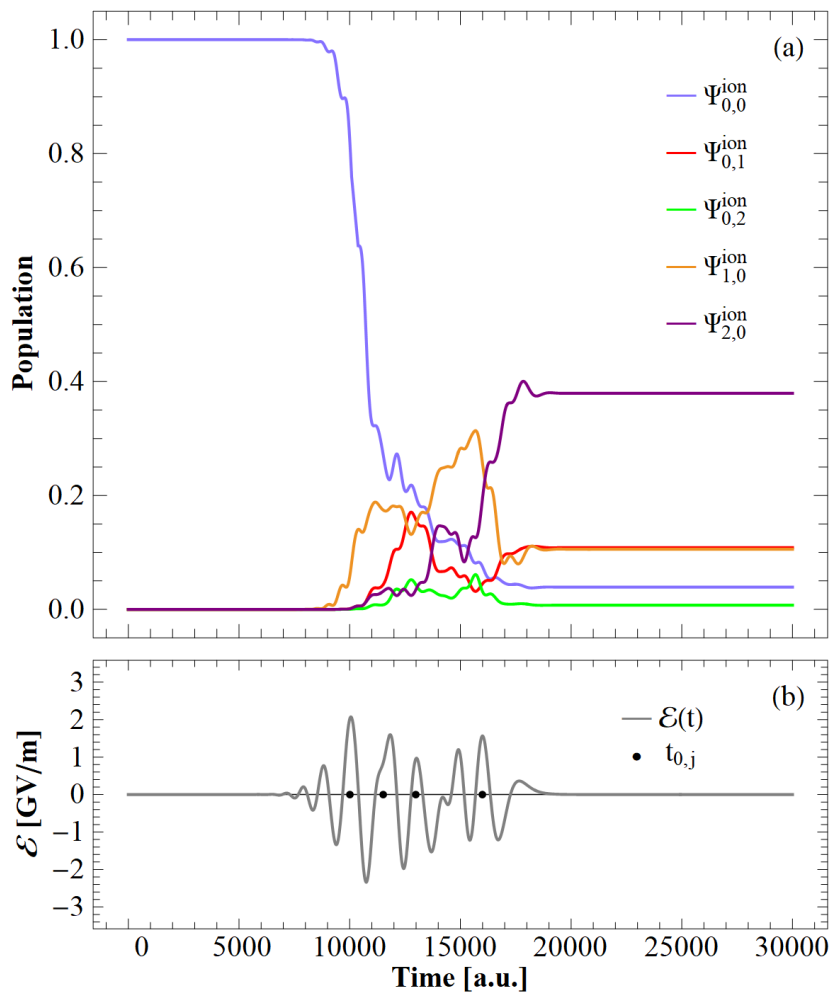
Table S1: Final populations of the vibrational eigenstates $\Psi^{\text{ion}}_{\nu_z,\nu_R}$, under the interaction of a sequence of two LCPs, as described in Table 2(a)

v_z	v_R	Population	v_z	v_R	Population	v_z	v_R	Population
0	0	0.4719	2	0	0.0643	4	0	0.0042
0	1	0.0088	2	1	0.0792	4	1	0.0024
0	2	0.0336	2	2	0.0183	4	2	0.0022
0	3	0.0143	2	3	0.0056	4	3	0.0003
0	4	0.0008	2	4	0.0103	4	4	0.0003
1	0	0.0494	3	0	0.0273			
1	1	0.1323	3	1	0.0219			
1	2	0.0281	3	2	0.0044			
1	3	0.0101	3	3	0.0036			
1	4	0.0044	3	4	0.0019			

Table S2: Final populations of the vibrational eigenstates $\Psi^{\text{ion}}_{\nu_z,\nu_R}$, under the interaction of a sequence of three LCPs, as described in Table 2(b)

v_z	v_R	Population	v_z	v_R	Population	v_z	v_R	Population
0	0	0.1575	2	0	0.1598	4	0	0.0001
0	1	0.0480	2	1	0.0337	4	1	0.0013
0	2	0.0490	2	2	0.0000	4	2	0.0033
0	3	0.0025	2	3	0.0013	4	3	0.0004
0	4	0.0097	2	4	0.0012	4	4	0.0001
1	0	0.3058	3	0	0.0028			
1	1	0.0292	3	1	0.0077			
1	2	0.1109	3	2	0.0057			
1	3	0.0528	3	3	0.0039			
1	4	0.0130	3	4	0.0003			

Table S3: Final populations of the vibrational eigenstates $\Psi^{\mathrm{ion}}_{\nu_z,\nu_R}$, under the interaction of a sequence of four LCPs, as described in Table 2(c)

v_z	v_R	Population	v_z	v_R	Population	v_z	v_R	Population
0	0	0.0390	2	0	0.3794	4	0	0.0070
0	1	0.1085	2	1	0.0662	4	1	0.0064
0	2	0.0073	2	2	0.0148	4	2	0.0007
0	3	0.0278	2	3	0.0094	4	3	0.0017
0	4	0.0080	2	4	0.0129	4	4	0.0004
1	0	0.1055	3	0	0.0354			
1	1	0.0117	3	1	0.0443			
1	2	0.0166	3	2	0.0173			
1	3	0.0344	3	3	0.0025			
1	4	0.0415	3	4	0.0011			